# Capillary Waves in Ionic Surfactant Solutions: Effects of the Electrostatic Adsorption Barrier and Analysis in Terms of a New Dispersion Equation

**ARTICLE** *in* THE JOURNAL OF PHYSICAL CHEMISTRY B · JUNE 2002

Impact Factor: 3.3 · DOI: 10.1021/jp012044f

# Capillary Waves in Ionic Surfactant Solutions: Effects of the Electrostatic Adsorption Barrier and Analysis in Terms of a New Dispersion Equation

**Francisco Monroy,* Mercedes G. Muñoz, José E. F. Rubio, Francisco Ortega, and Ramón G. Rubio**

*Department Química Física I, Facultad de Química, Universidad Complutense, E28040-Madrid, Spain*

*Received: May 30, 2001; In Final Form: March 5, 2002*

We have studied the dispersion of capillary waves on the surface of aqueous solutions of the cationic surfactant dodecylammonium chloride (DAC) by using surface quasi-elastic light scattering (SQELS) combined with equilibrium surface tension measurements. To test the role of electrostatics on the dynamical behavior of the adsorbed surfactant monolayer at the air/solution interface, experiments in absence and presence of an inert electrolyte (KCl) have been performed. The equilibrium results have been analyzed in terms of the Frumkin−Davies equation of state. For the salt-free system, the Lucassen−van den Tempel model describes the dilational viscoelasticity results provided that the effects of adsorption barrier are accounted for. In contrast, when inert electrolyte is added, the viscoelastic behavior is anomalous, and negative apparent dilational viscosities are obtained. A new dispersion equation is proposed that accounts for internal coupling between capillary and dilational modes and leads to nonanomalous dilational viscosities.

## Introduction

Monolayers of adsorbed amphiphiles are important as models of two-dimensional systems and because of their relevance for problems of practical interest as foaming or emulsification.[1,2] Surfactant monolayers adsorbed at the water−air interface have been found to support several rheological modes at equilibrium and to present viscoelastic character.[3] Most frequently, the contribution of the shear modes to the elastic moduli is smaller than that from compression modes.[4,5] Although capillary and longitudinal motions are the most important ones for thin adsorbed monolayers of small monomeric amphiphiles,[5] other modes (e.g., bending and splay) may be important for thicker monolayers.[6]

The work of Levich on surface hydrodynamics[7] established the physical grounds for studying the motion of thin viscoelastic monolayers adsorbed at fluid interfaces. For arbitrary transversal ($u_z$) and longitudinal ($u_x$) harmonic deformations of the interface, the elastic free-energy functional can be written as[5−7]

$$\delta F = \frac{1}{2}\gamma\left(\frac{\partial u_z}{\partial x}\right)^2 + \frac{1}{2}\tilde{\epsilon}\left(\frac{\partial \mathrm{u_x}}{\partial \mathrm{x}}\right)^2 \qquad (1)$$

In thin monolayers, capillary waves are controlled by the equilibrium surface tension, $\gamma = \gamma_{eq}$, which acts as a restoring force for small-amplitude out-of-plane deformations of the interface with respect to the flat equilibrium shape. In addition, no transversal dissipation must be assumed to exist well below the hydrodynamic limit, that is, for deformations with spatial range sufficiently larger than the monolayer thickness.[6−9]

The dilational waves are characterized by a complex elastic modulus:

$$\tilde{\epsilon}(\omega) = \epsilon(\omega) + i\omega\kappa(\omega) \qquad (2)$$

where $\epsilon(\omega)$ is the dynamic elasticity, and $\kappa(\omega)$ is the dilational viscosity, both accounting for the linear viscoelastic response of the interface to an in-plane dilation, $\partial u_x \sim \delta$A, driven by surface tension gradients, $\delta\gamma$:[3,5,7]

$$\delta\gamma = \tilde{\epsilon}\frac{\partial u_x}{\partial x} = \tilde{\epsilon}\frac{\mathrm{d}A}{A} \qquad (3)$$

For soluble monolayers where material exchange between the bulk solution and the interface happens, any dilation $\delta A$ induces a surface concentration change, $\delta\Gamma$, which is in general smaller than it would be for an insoluble film (Langmuir film). However, if a soluble Gibbs monolayer is compressed at a high enough frequency, it behaves as insoluble; in this case $\epsilon(\omega) = \epsilon_0$, $\epsilon_0$ being the Gibbs elasticity.

In general, the dilational parameters are frequency-dependent, and the $\epsilon$ and $\omega\kappa$ versus bulk surfactant concentration, $c$, curves are expected to show a peak at the concentration at which compression and dissolution rates are comparable.[3] The first predictive model for the viscoelastic behavior of soluble monolayers was that of Lucassen and van den Tempel (LT).[9,10] They assumed that the material exchanges between the bulk and the surface are governed by Fickian's diffusion:[10]

$$\tilde{\epsilon}(\omega) = \epsilon(\omega) + i\omega\kappa(\omega) = \epsilon_0\frac{(1+\Omega)+i\Omega}{1+2\Omega+2\Omega^2} \qquad (4)$$

where the adimensional parameter $\Omega$ is given by

$$\Omega = \sqrt{\frac{1}{\omega\tau_{\mathrm{dif}}}} \text{ with } \tau_{\mathrm{dif}} = \frac{2}{D}\left(\frac{\mathrm{d}\Gamma}{\mathrm{d}c}\right)^2 \qquad (5)$$

$\tau_{dif}$ is the characteristic time of the diffusive exchange between the monolayer and the subsurface, $D$ is the bulk surfactant diffusion coefficient, and $\Gamma$ is the surface concentration.

In general, there is a good agreement between the predictions of the LT model and the experimental results for nonionic surfactant solutions.[11] However, significant discrepancies have

* To whom correspondence should be addressed.

10.1021/jp012044f CCC: $22.00 
Published on Web 05/11/2002

been found for ionic surfactants.[12,13] If an adsorption barrier exists (e.g., the electrostatic barrier built-in adsorbed monolayers of ionic surfactants), diffusion is not the only factor controlling the material exchanges involved in the adsorption dynamics; thus, new kinetic contributions must be taken into account in the dynamic equations.

Prosser and Franses[14] and Datwani and Stebe[15] have reviewed in detail the influence of the electrostatics on the adsorption dynamics of ionic surfactants. To model the system, it is necessary to use an equation of state and either to solve numerically the Nernst−Planck diffusion−migration equation[16] or to assume that quasi-equilibrium exists within the double-layer limits.[13,15,16] The overall picture drawn from the work of MacLeod and Radke[16] indicates that both the equilibrium adsorption and the adsorption dynamics may be rationalized in terms of the magnitudes of the electrical double-layer thickness (gauged by the Debye length), and the adsorption layer thickness, which corresponds to the characteristic distance over which surfactant concentration changes occur in the bulk solution during the adsorption process.

The effect of electrostatics on the viscoelastic moduli (dilational elasticity $\epsilon$ and viscosity $\kappa$) has received less attention than the dynamic surface tension. Bonfillon and Langevin[13] have carried out low-frequency longitudinal wave experiments for monolayers of sodium dodecyl sulfate, SDS, at the interface between water and *n*-dodecane. Their results indicate that, in the absence of inert electrolytes, the effects of the electrical double layer play a fundamental role in the description of the exchange of surfactant ions between the bulk and the interface. However, in the presence of a high concentration of inert electrolyte, the results can be described by adsorption models that do not include explicitly the existence of ions. More recently, Warszynski et al.[17] have also discussed the surface elasticity of ionic surfactant solutions, reaching similar conclusions.

Despite the reasonable agreement between theory and experiments described in refs 13 and 17 for some systems, other ionic surfactant solutions present a striking viscoelastic behavior. In effect, Earnshaw and McCoo[18] and Monroy et al.[19] have found negative *apparent* dilational viscosities from electrocapillary wave experiments on solutions of cetyl trimethylammonium bromide (CTAB). Negative apparent dilational viscosities have also been obtained from the analysis of capillary wave experiments on insoluble monolayers.[20−23] Most probably, these striking results arise from deficiencies in the hydrodynamic description of the interface.[8] This is a problem because, to test adsorption models in the medium- and high-frequency ranges, the experimental data of $\epsilon(\omega)$ and $\kappa(\omega)$ are frequently obtained from capillary wave experiments. In this process, it is absolutely necessary to use an appropriated dispersion equation of the interface, otherwise the viscoelastic moduli calculated might be affected by artifacts.

In this paper, we report on the high-frequency behavior of the dilational elasticity and the viscosity of the surface of dodecylammonium chloride (DAC) solutions, in the absence and in the presence of an inert electrolyte (KCl). The behavior of bulk solutions of DAC has been studied previously.[24,25] Motumura et al. have reported equilibrium surface tension data, $\gamma_{eq}$, for solutions of DAC in water.[26] They observe a small kink in the $\gamma_{eq}$ versus solution concentration, $c$, isotherm at $c \sim 1.4$ mM, suggesting the existence of a gas-to-liquid expanded-phase transition. Recently, Kizling et al. have carried out SQELS experiments in the same system.[27] However, their analysis of the SQELS spectra in terms of the dispersion equation is not conclusive: (a) The authors use the $\gamma_{eq}$ data of Motumura et al.[26] despite the convenience of measuring $\gamma_{eq}$ for the same sample that the SQELS spectra has been already stressed.[6] (b) Instead of obtaining $\kappa(\omega)$ from the fits of the experimental spectra, the authors "rely upon the data of Byrne and Earnshaw[28] for monolayers of myristic acid", which is a noncharged and near-insoluble surfactant. (c) Finally, they assume $\epsilon(\omega) = \epsilon_0$ and calculate $\epsilon_0$ from the Gibbs adsorption equation. For this purpose, they consider ideal solution behavior (i.e., activities equal to surfactant concentration). Under the above conditions, Kizling et al.[27] found some quantitative disagreements between the calculated and experimental spectral frequencies and widths. In the present work, $\gamma(\omega)$, $\epsilon(\omega)$, and $\kappa(\omega)$ will be obtained from the analysis of the experimental spectra using the full theoretical expression derived from the hydrodynamic dispersion equation.[3,7] As it will be shown, in the absence of inert electrolyte, positive values of $\kappa(\omega)$ are found. However, for the DAC + water + KCl (60 mM) system, anomalous dilational viscosities are reported. This anomalous result suggested us to modify the classical dispersion equation by introducing an internal coupling between the capillary and dilational motions. This extended dispersion equation allows us to explain the SQELS data without using negative effective values of the dilational viscosity.

## Experimental Section

DAC was synthesized from previously distilled dodecylamine (Aldrich RPE) dissolved in benzene by bubbling "in situ" prepared HCl under continuous stirring. The product was recrystallized in benzene until no amine was found, and the purity was checked by spectroscopic (FTIR and NMR) and calorimetric (DSC) methods. In pure water, the CMC was determined by conductimetry and surface tension measurements, obtaining a value close to 13 mM, in agreement with previously reported data.[29] KCl was Carlo Erba RPE, with purity >99% and was dried under vacuum at 373 K shortly before use. Bidistilled and deionized water was freshly prepared before use in a Milli-Q unit, its purity being tested by conductivity measurements (the resistance was larger than 19 MΩ cm).

The apparatus used for measuring the spectra of the light scattered by thermally excited capillary waves (SQELS) has been described in previous works.[29,31] It has been calibrated using pure liquids (*n*-hexane, ethanol, dimethyl ether, and water) and can be used in the wavevector range $100 \leq q\ (\mathrm{cm}^{-1}) \leq 900$. Both the autocorrelation functions and the power spectra of the light scattered by thermally excited capillary waves can be simultaneously measured.

## Surface Hydrodynamics. Dispersion Equation

For a monolayer-covered surface, the propagative parameters $\omega$ and $q$ of the surface modes are related to the constitutive properties through the dispersion equation, $D(\omega) = 0$. In a thin monolayer at the air−water interface in which capillary and dilational modes are the only important ones: [3,7]

$$D(\omega) = L(\gamma)\cdot T(\tilde{\epsilon}) - C(\rho,\eta) \equiv 0 \tag{6}$$

where

$$L(\tilde{\epsilon}) = \tilde{\epsilon}q^2 + i\omega\eta(q+\mu) \tag{7}$$

$$T(\gamma) = \gamma q^2 + i\omega\eta(q+\mu) - \frac{\rho}{q}\omega^2 + \rho g \tag{8}$$

with $\rho$ and $\eta$ being the liquid density and viscosity, respectively,

and $\mu^{-1}$ is the capillary penetration depth:

$$\mu^2 = q^2 + i\omega\frac{\rho}{\eta} \text{ with } \mathrm{Re}(\mu) > 0 \tag{9}$$

and $C(\rho,\eta)$ the coupling constant is

$$C(\rho,\eta) = [i\omega\eta(q-\mu)]^2 \tag{10}$$

which accounts for hydrodynamic coupling between the capillary and the dilational modes.

The spectrum of the scattered light by thermally excited capillary waves is given by

$$P_z(q;\omega) = -\frac{2k_BT}{\pi\omega}\mathrm{Im}\left[\frac{\tilde{\epsilon}q^2 + i\omega\eta(q+\mu)}{D(q,\omega)}\right] = -\frac{2k_BT}{\pi\omega}\mathrm{Im}\left[\frac{L(\tilde{\epsilon})}{D(q;\omega)}\right] \tag{11}$$

However, it is known that experimental spectra appear more or less broadened because of instrumental contributions and that the experimental spectra correspond to a convolution between the theoretical spectrum and an instrumental function, $G(\omega)$. In our experimental technique, $G(\omega)$ can be accurately described by a Gaussian function.[29] Consequently, the constitutive parameters $\gamma(\omega)$, $\epsilon(\omega)$, and $\kappa(\omega)$ must be obtained from the experimental spectra by fitting

$$P_q(\omega) = \int P_z(q,\omega)G(\omega)\mathrm{d}\omega \tag{12}$$

In practice, this convolution is performed by Fourier transformation: $P_q(\omega) = \mathrm{FT}^{-1}\{\mathrm{FT}[P_z(q,\omega)]\ \mathrm{FT}[G(\omega)]\}$, where $\mathrm{FT}^{-1}$ denotes the inverse transform.

## Results

Figure 1 shows the equilibrium surface tension values, $\gamma_{eq}$, for the DAC + water system at 298.15 and 308.15 K. The results at 298.15 K are in good agreement with those reported by Motumura et al.[26] The value of the CMC, observed at a concentration of DAC ca. 13 mM, is also in agreement with that reported by Dorshow et al.[30] As it can be seen, the temperature slightly modifies the behavior of $\gamma_{eq}$, specially in the range $c <$ CMC. The near-linear part of the isotherms, just before the CMC, has a larger slope for the higher temperature. This points out a decrease of surface density $\Gamma$ with increasing $T$. More important changes are introduced by modifying the ionic strength. We have tentatively chosen [KCl] = 60.0 mM because the second osmotic virial coefficient for the micellar solution, measured by light scattering at the same electrolyte concentration, is near zero,[25] that is, the attractive and the repulsive interactions compensate each other.

Figure 2a shows some of the SQELS spectra obtained at $q = 211.3\ \mathrm{cm}^{-1}$ and 298.15 K for different concentrations of the DAC + water system. The spectra are well fitted by Voigt functions, which means that $P_q(\omega)$ can be approximately described by a Lorentzian function. As an example, Figure 2b shows the $q$-dependence of the spectra for a surfactant concentration $c = 5.9$ mM in the DAC + water + KCl (60.0 mM) system. As expected,[5] increasing $q$ reduces the intensity of the spectra ($I_z \sim k_BT/\gamma q^2$), while the central peak frequency and its width increase, that is, both capillary propagation frequency and damping, increase with $q$. Figure 3 shows the maximum frequency, $\omega_C$, and the half-height width, $\Delta\omega_C$, obtained by fitting the experimental spectra to a Voigt function. The change of slope observed for the $\omega_C$ versus $c$ curves follows the variation of $\gamma_{eq}$ with concentration, showing a slope break at $c \sim 1.4$ mM coinciding with the region of the gas-to-liquid expanded phase transition proposed by Motumura et al.[26] A similar behavior of $\omega_C$ has been reported by Kizling et al.[27] for solutions of DAC at the same temperature and at a single $q = 534\ \mathrm{cm}^{-1}$.

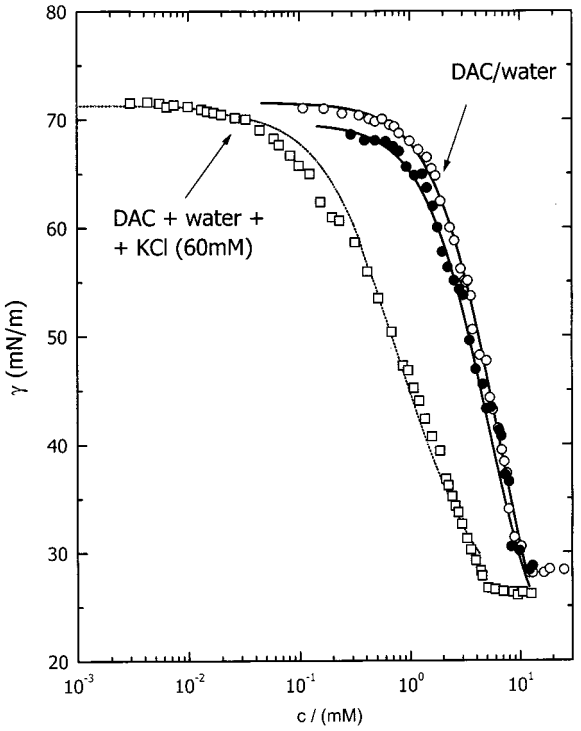


**Figure 1.** Equilibrium surface tension $\gamma$ for DAC solutions as a function of surfactant concentration $c$. Symbols are experimental results: (○) DAC + water at 298.15; (●) DAC + water at 308.15; and (□) DAC + water + KCl 60 mM at 298.15. The thick lines correspond to the fits to the Frumkin−Davies equation of state (eq 16) with the following parameters: $K = 130\ \mathrm{m}^3/\mathrm{mol}$, $H = 2RT$, and $A_0 = 39\ \mathrm{Å}^2$ for $T = 298$ K, and $A_0 = 48\ \mathrm{Å}^2$ at 308 K. The dotted line has been calculated for the system with [KCl] = 60 mM using the same energetic parameters obtained for the system without inert electrolyte and $A_0 = 34\ \mathrm{Å}^2$.

The concentration dependence of $\Delta\omega_C$ is more complex. Two maxima are observed, more clearly at the highest $q$. Kizling et al.[27] reported only one maximum centered ca. 2 mM, although they did not report any data below 0.2 mM, where a low-concentration maximum is present in our data. The high-concentration maximum appears at a value of $c$ slightly above the phase transition suggested by Motumura et al.[26] Only at very low concentration, $c < 0.01$ mM, are the values observed for $\Delta\omega_C$ close to that of the pure solvent, increasing then abruptly until the first maximum at $c \sim 0.1$ mM is reached. The surface tension remains in a value close to that for pure solvent ($\gamma_0 \sim 72.1$ mN/m), even for much higher concentrations ($c \sim 2$ mM), where the second maximum appears. Similar features are observed in the presence of salt, [KCl] = 60 mM (see Figure 3d). The main difference is that now only one broad maximum appears. The wave damping is larger than for the free surface of the pure solvent, even at concentrations below $10^{-4}$ mM, where $\gamma = \gamma_0$.

A rough analysis of the results can be performed in terms of the limit solutions of the classical dispersion equation (setting

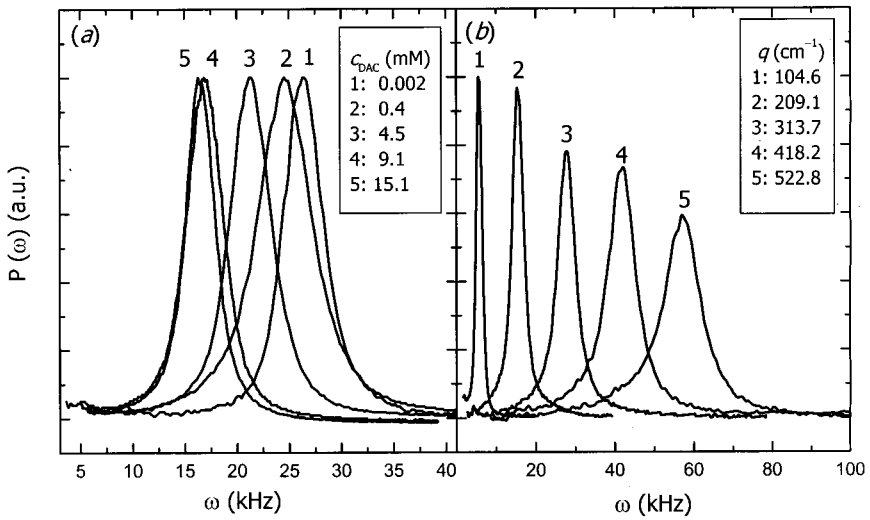


**Figure 2.** Experimental spectra of the light scattered by thermal capillary waves in DAC solutions. (a) effect of surfactant concentration for the DAC + water system at $q = 209.2$ cm$^{-1}$ and 298.15 K. (b) Effect of the wavevector for the DAC ($c = 5.9$ mM) + water + KCl (60 mM) solution at 298.15 K. The shape of the spectra can be accurately described by a Voigt function, i.e., the spectra of the scattered light can be approximated by a Lorentzian function (see eq 12).

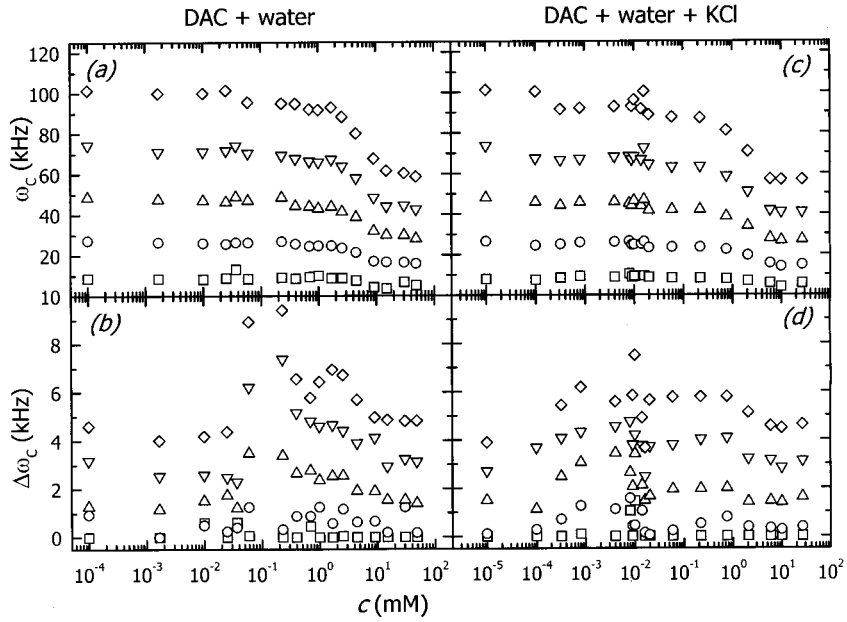


**Figure 3.** Concentration dependence of the characteristic frequency of the SQELS spectra $\omega_C$ and the width at half-height $\Delta\omega_C$. (a) and (b) correspond to the DAC + water system, and the symbols correspond to different values of $q$ (in cm$^{-1}$): (□) 104.6; (○) 209.1; (△) 313.7; (▽) 418.2; (◇) 522.8. (c) and (d) correspond to the system DAC + water + KCl (60 mM) system, and the symbols correspond to the same values of $q$ as in (a).

$\epsilon = \omega\kappa = 0$ in eqs 6−10). Under these conditions, a simple relationship exists between the propagation frequency, $\omega_C$, and surface tension (Kelvin's law), as well as between the wave damping, $\Delta\omega_C$, and the viscosity of the subphase (Stokes' law):

$$\omega_C \approx (\gamma/\rho)^{1/2} q^{3/2} \tag{13}$$

$$\Delta\omega_C \approx 2(\eta/\rho) q^2 \tag{14}$$

Figure 4 shows the $q$-dependence of $\omega_C$ and $\Delta\omega_C$ at different surfactant concentrations, both with and without salt. $\omega_C$ follows quite closely the $q^{3/2}$-dependence predicted by Kelvin's law, although the apparent values of the surface tension, obtained from the slope of the linear $\omega_C$ versus $q^{3/2}$ representation, are systematically lower than the equilibrium ones, $\gamma_{eq}$, this being more pronounced in the case of added electrolyte (KCl 60 mM). This means that although the transversal mode propagates as a pure capillary-like one ($\omega_C \sim q^{3/2}$), it is affected by significant dilational effects (i.e., $\epsilon$ and $\omega\kappa \neq 0$). As a consequence, the experimental $\Delta\omega_C$ values are always higher than the ones predicted by Stokes' law (see Figure 4c−d). This indicates that extra dissipative effects from dilational motion exist within the film, that is, the surfactant monolayer has viscoelastic character.

## Discussion

**Equilibrium Behavior: Surface Equation of State.** It is well established that electrostatic interactions should be incorporated to any realistic model of ionic surfactant equilibrium adsorption at the air−solution interface.[12−17] Davies and Rideal[32] proposed an ES that accounts for the decrease in surfactant adsorption because of the electrostatic surface potential $\Psi_0(\Gamma)$,

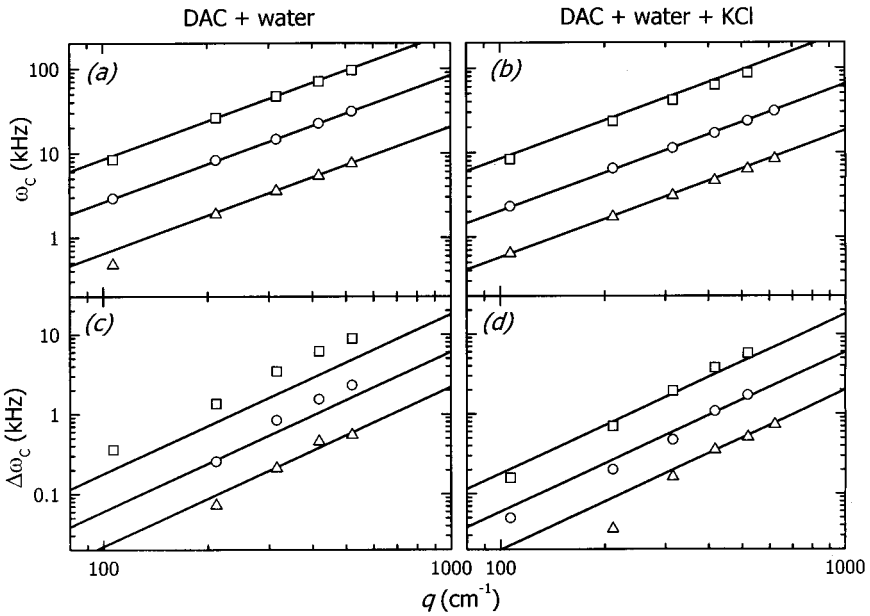


**Figure 4.** (a) Wavevector dependence of $\omega_C$ for three different surfactant concentrations. DAC + water system: (□) 0.06 mM; (○) 1.68 mM; (△) 9.1 mM. (b) same for the DAC + water + KCl (60.0 mM): (□) 0.06 mM; (○) 2.06 mM; (△) 5.90 mM. The $q$ dependence of the capillary wave damping, $\Delta\omega_C$, in absence and presence of salt (KCl 60 mM) is shown in (c) and (d), respectively; the symbols refer to the same surfactant concentrations as in (a) and (b), respectively. The continuous lines correspond to the predictions of the limit ideal laws in eqs 13 and 14. For the sake of clarity, the points marked with (○) and (△) have been shifted toward lower $\omega_C$'s.

generated by the charged adsorbed monolayer:

$$\frac{\Gamma}{\Gamma_\infty - \Gamma} = aK \exp\left(\frac{2H}{RT}\frac{\Gamma}{\Gamma_\infty}\right)\exp\left(-\frac{zF\Psi_0}{RT}\right) \qquad (15)$$

In this ES, known as the Frumkin−Davies (FD) adsorption equation, $a$ is the surfactant activity in the solution and $z$ is its charge; $K$ is the equilibrium constant of the adsorption/desorption process, and $F$ is the Faraday constant. As in the Frumkin's ES, the energetic parameter $H$ accounts for nonideal lateral specific interactions between neighbor adsorbed molecules: $H > 0$ for cohesive interactions (cooperative adsorption), and $H < 0$ in the repulsive case (anticooperative adsorption).

Assuming the Goüy−Chapman distribution for the ions present in the subsurface, $c_i = c_i^0 \exp(-zF\Psi_0/RT)$, Borwankar and Wasan obtained the following expression for the $\gamma-a$ isotherm:[33]

$$\frac{\gamma_0 - \gamma(a)}{RT} = -\Gamma_\infty\left[\ln(1-\theta) + \frac{H}{RT}\theta^2\right] + \frac{1}{4\zeta^{-1}\lambda}\left[\cosh\left(\frac{F\Psi_0}{2RT}\right) - 1\right] \qquad (16)$$

where $\theta = \Gamma/\Gamma_\infty$, $\zeta^{-1} = F^{-1}\,(\epsilon_0\epsilon RT/2I)^{1/2}$ is the Debye length, $I$ is the ionic strength, and $\lambda$ is the Bjerrum length, $\lambda = e^2/4\pi\epsilon_0\epsilon k_B T$ ($\lambda \sim 7$ Å for monovalent ions in water at 25 °C). It must be stressed that the effect of Coulombic interactions appears in the two terms of eq 16 since the coverage fraction $\theta$ depends on the surface potential $\Psi_0$ (and vice versa) through eq 15.

To fit the experimental $\gamma$ versus $c$ data to the FD isotherm, we have calculated activities using the Debye−Hückel approximation.[34] The results of these fits are represented in Figure 1. In all cases the $A_0 = 1/\Gamma_\infty$ values obtained from the fits are in a quantitative agreement with those obtained directly from the Gibbs' adsorption law and are similar to those reported for other ionic surfactants.[35] The value $A_0 \sim 39$ Å$^2$ (DAC + water at 298.15 K) corresponds to an ionic head radius of ca. 3.5 Å, close to the hydrated radii found for a variety of ions in aqueous solution.[36,37] When the temperature is increased to 308.5 K, the ionic head radius increases to 4.0 Å, as found for single ammonium ions in solution because of entropic reasons.[37] Using Gibbs' equation for the system with KCl and assuming full counterion condensation, one obtains from the final slope of the isotherm a value of $A_0$ ($= 1/\Gamma_\infty$) $\sim 34$ Å$^2$, in excellent agreement with the value obtained from FD equation.

Within their uncertainty, the values of $K$ (130 m$^3$/mol) and $H$ ($2RT$) can be considered as temperature and ionic strength independent for the three curves (in fact a slightly better fit is obtained at 308 K with $K = 155$ m$^3$/mol). A similar conclusion for $K$ has been reached by Prosser and Franses in the anionic surfactant system SDS + water with and without inert electrolyte,[14] and is consistent with the unspecific character of the hydrophobic surfactant−interface interaction. The approximate constancy of $H$ seems also consistent with the fact that it deals with the interactions between the hydrophobic tails of the surfactant at the surface, and the electrostatic interactions are taken into account by the Gouy−Chapman distribution.

The parameters of the FD isotherm allow one to make a qualitative sketch of the surface of the DAC solutions. In effect, as discussed by MacLeod and Radke[16] and by Datwani and Stebe,[15] the Debye length $\zeta^{-1}$ can be taken as a measure of the thickness of the electrical double layer. At the CMC, $\zeta^{-1} = 31$ Å for the system without KCl, while $\zeta^{-1} = 12$ Å for [KCl] = 60 mM. On the other hand, $\Gamma_\infty/c^\infty$ (with $c^\infty$ being the surfactant concentration far from the interface) gauges the thickness of the adsorption layer; thus, $\Lambda = \Gamma_\infty/(c^\infty\kappa)$ may be considered as a ratio of the adsorption thickness to the Debye length. In our systems, for the $c$ equal to the CMC, $\Lambda$ ranges from 140 to 400 for the systems without and with inert electrolyte, respectively, which are of the same order as the value used by MacLeod and Radke in their simulations. The noticeable reduction of the thickness of the electrical double layer explains why the effects of electrostatics on the adsorption dynamics seem to be more

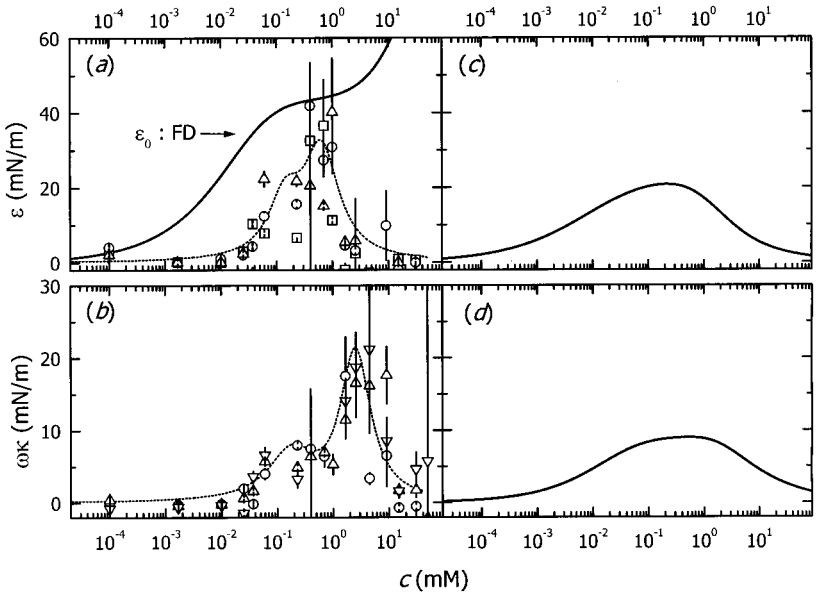


**Figure 5.** (a) Dilational elasticity modulus $\epsilon(\omega)$ for the DAC + water system at different $q$'s calculated from the best fits of the experimental SQELS spectra to the theoretical profile (eqs 11 and 12) given by the classical dispersion equation (eq 6). The symbols refer to different values of $q$ (in $cm^{-1}$): (□) 209.1; (○) 313.7; (△) 418.2; (▽) 522.8. The dotted line is a guide to the eyes. The curve marked FD in (a) corresponds to the equilibrium elasticity (compression modulus $\epsilon_0$) calculated with the Frumkin−Davies (FD) equation of state with the parameters of Figure 1. (b) Dilational loss modulus $\omega\kappa(\omega)$. The symbols and the line have the same meaning as in (a). The figures at the right ((c) and (d)) show the predictions of the dynamic dilational viscoelasticity from the Lucassen−van den Tempel model (LT) calculated for a value of the diffusion coefficient $D = 5 \times 10^{-6}$ $cm^2/s$ and the equilibrium values of $\epsilon_0$ and $(d\Gamma/dc)_{eq.}$ obtained from the FD equation of state.

important in the absence of inert electrolytes. However, as it will be seen below, the anomalous negative dilational viscosities are found for the DAC solutions with [KCl] = 60 mM.

**Dynamic Behavior.** *DAC Solutions without Inert Electrolyte.* The fit of the experimental spectra to eqs 11−12 allows to determine $\gamma(\omega)$, $\epsilon(\omega)$, and $\kappa(\omega)$ for these monolayers. We have found $\gamma(\omega) \approx \gamma_{eq}$ within the uncertainty of $\gamma(\omega)$; this means that for the present frequency range $\gamma$ is fully relaxed, that is, capillary motion is governed by the equilibrium surface tension.[3] Figure 5a shows the concentration dependence of $\epsilon(\omega)$ obtained for three different $q$'s, corresponding to a frequency range 50−100 kHz. As expected for soluble systems, we observe a broad maximum,[10] which is located at a concentration ca. 0.5 mM. The two maxima in the $c$-dependence of the capillary damping ($\Delta\omega_C$ vs $c$ curve in Figure 4), can be explained now in terms of the shape of the $\epsilon(\omega)$ versus $c$ curve. In effect, maximum capillary damping should correspond to resonance between capillary and dilational modes. This resonance happens for $\epsilon/\gamma \sim 0.16$, a condition which is reached for two different concentrations in our system: at $c_1 \sim 0.1$ mM and $c_2 \sim 2$ mM.

Figure 5a shows that there are significant differences between the dynamic values of $\epsilon(\omega)$ and its equilibrium value $\epsilon_0$ calculated from the FD equation of state ($\epsilon(\omega) < \epsilon_0$) pointing out the soluble character of this monolayer in this frequency range. Figure 5c and 5d shows respectively the calculated values of $\epsilon(\omega)$ and $\omega\kappa(\omega)$ obtained for the DAC + water system using the LT model with $\epsilon_0$ calculated from the FD equation of state. The maxima in the $\epsilon(\omega)$ and $\omega\kappa(\omega)$ experimental data roughly coincide with the ones predicted from the LT model. However, the experimental $\omega\kappa(\omega)$ versus $c$ curve is not well explained by the LT−FD model that predicts values smaller than the experimental ones at high concentrations (1 mM < $c$ < CMC). To explain this fact, one may invoke the existence of an adsorption barrier.[38] Liggieri et al.[39,40] have shown that the diffusion-kinetic adsorption mixed mechanism can be accurately described by a renormalized diffusion kinetics where the adsorption barrier is accounted for by an effective diffusion coefficient:

$$D_{eff} = D \exp\left(-\frac{e\Psi_0}{RT}\right) \tag{17}$$

Figure 6a shows also a simulation of the dilational viscoelasticity by using this effective diffusion coefficient that depends on the surfactant concentration through $\Psi_0$. As it can be observed, two separated maxima are now predicted for the loss modulus $\omega\kappa(\omega)$, although the quantitative agreement with the experimental results is not better than the previous one.

The group of Langevin has proposed a model for dilational viscoelasticity that takes into account an adsorption barrier that slows down the adsorption−desorption fluxes.[41] According to this modified version of the Lucassen−van den Tempel model (MLT model), the viscoelastic modulus can be written as

$$\tilde{\epsilon}(\omega) = \epsilon_0 \frac{\frac{1}{2\Omega} + i\left(\frac{1}{2\Omega} + \frac{\omega}{k_D}\right)}{\left(1 + \frac{1}{2\Omega}\right) + i\left(\frac{1}{2\Omega} + \frac{\omega}{k_D}\right)} \tag{18}$$

where $k_D$ is the kinetic constant for the desorption process, which is related to the adsorption equilibrium constant, $K \equiv k_A/k_D \sim (d\Gamma/dc)_{eq}$. The expression for the viscoelastic modulus in eq 18 reduces to the LT equation (eqs 4 and 5) when no barrier exists ($k_D \rightarrow \infty$).

Since the characteristic time for desorption is given by $\tau_{des} = k_D^{-1}$, this expression can be rewritten in terms of a new reduced parameter, $\Sigma \equiv \omega\tau_{des} = \omega/k_D$; after some algebra one finds:

$$\tilde{\epsilon}(\omega) = \epsilon + i\omega\kappa = \epsilon_0 \frac{[(1+\Omega) + 2\Omega\Sigma(1+\Omega\Sigma)] + i[\Omega(1+2\Omega\Sigma)]}{1 + 2\Omega(1+\Sigma) + 2\Omega^2(1+\Sigma^2)} \tag{19}$$

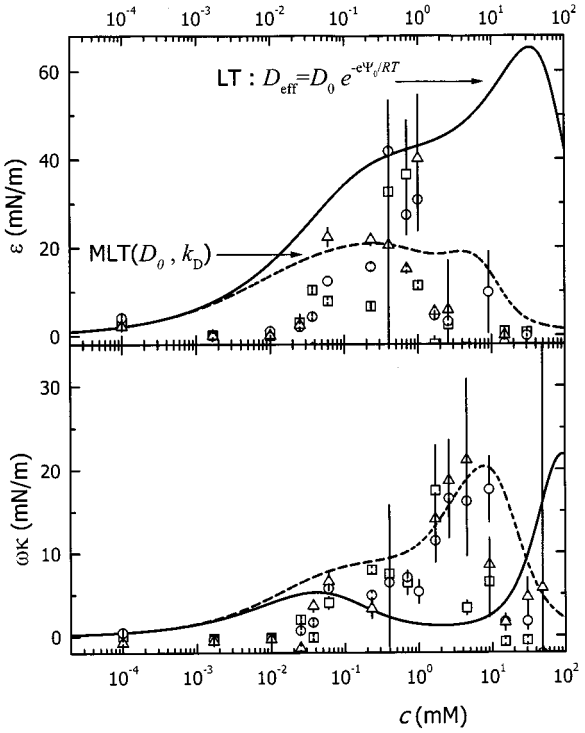


**Figure 6.** Dynamic elasticity and loss modulus for the DAC + water + KCl system. The symbols are the same experimental data as Figure 5. The continuous lines represent the predictions of the LT model with an effective diffusion coefficient given by eq 17 and $D = 5{\cdot}10^{-6}$ cm$^2$·s. $\epsilon_0$ and $(d\Gamma/dc)_{eq}$ have been calculated from the Frumkin−Davies equation of state with the parameters of Figure 1. The dashed lines give the predictions of the Lucassen−van den Tempel model modified by Langevin and co-workers (MLT model) to include the effects of an adsorption barrier (eq 18).

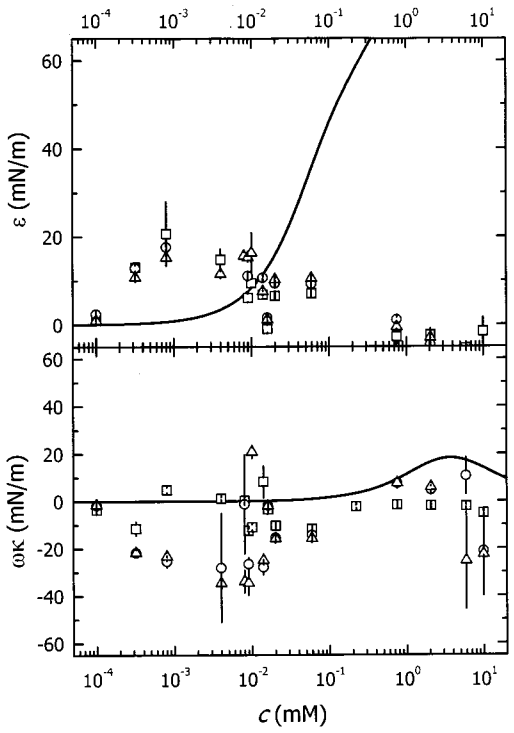


**Figure 7.** (a) Dilational elasticity modulus $\epsilon(\omega)$ for the DAC + water + KCl system at different $q$'s calculated from the best fits of the SQELS spectra to the theoretical profile (eqs 11 and 12) given by the classical dispersion equation (eq 6). The symbols refer to different values of $q$ (in cm$^{-1}$): (□) 209.1; (○) 313.7; (△) 418.2; (▽) 522.8. The dotted line is a guide to the eyes. The curve marked FD in (a) corresponds to the equilibrium elasticity (compression modulus, $\epsilon_0$) calculated with the Frumkin−Davies (FD) equation of state with the parameters of Figure 1. (b) Dilational loss modulus $\omega\kappa(\omega)$. The symbols and the line have the same meaning as in (a). The values of the loss modulus obtained from the fits of the SQELS spectra to the classical dispersion equation have to be taken as apparent values.

If adsorption and desorption are activated processes, the adsorption dynamics is controlled by the surface potential, which strongly reduces the adsorption−desorption rates: $k_A = k_A^{(0)} \exp(-F\Psi_0/RT)$ and

$$\Sigma = \frac{\omega}{k_D} = \frac{\omega}{k_A}\left(\frac{d\Gamma}{dc}\right)_{eq} = \frac{\omega}{k^{(0)}_A} e^{F\Psi 0/RT}\left(\frac{d\Gamma}{dc}\right)_{eq} \qquad (20)$$

Li et al.[42] have measured the adsorption−desorption rate constants for a variety of cationic surfactants: the adsorption constant, $k_A$, varies strongly with chain length, while the desorption constant, $k_D$, is near constant and independent of the surfactant, $k_D \sim 5 \times 10^{-4}$ mol m$^{-2}$ s$^{-1}$. The characteristic equivalent frequency $k = (k_A c + k_D)/\Gamma_\infty$ was found to depend mainly on surfactant concentration but not on its nature and to be about 100 s$^{-1}$ for $c = 1$ mM and 500 s$^{-1}$ for $c = 4$ mM. By using these values of the characteristic adsorption frequency and the bulk diffusion coefficient, $D = 5 \times 10^{-6}$ cm$^2$/s, we have obtained $\epsilon(\omega)$ and $\omega\kappa(\omega)$ from the modified MLT model (eqs 19 and 20). As it can be observed in Figure 6 (dashed line), the agreement with the experimental values of the dilational viscoelasticity is quite satisfactory.

*DAC Solutions with Inert Electrolyte.* More striking is the situation found for the DAC + water system when inert electrolyte (60 mM KCl) is added. As shown by Figure 7, in the low-concentration range where adsorption is very small ($\gamma_{eq} \sim \gamma_0$), negative values of $\kappa(\omega)$ are obtained, while $\epsilon(\omega)$ shows a broad maximum in the same region. The theoretical prediction from the MLT model fails: for $c \sim 10^{-3}$ mM, the experimental values of $\epsilon(\omega)$ show a maximum close to 20 mN/m, while the MLT value remains close to zero. For concentrations up to $10^{-3}$ mM, where $\gamma - \gamma_0 \leq 0.1$ mN/m, one obtains $\epsilon_0 \leq 1$ mN/m, as expected for a diluted monolayer. More important discrepancies are shown by the loss modulus $\omega\kappa(\omega)$; the MLT prediction remains close to zero up to 0.1 mM, while the experimental data show negative apparent values.

To explain negative values of $\kappa(\omega)$, Earnshaw et al.[20] and Sharpe and Eastoe[23] have made use of the theoretical results of Velarde et al.[43,44] However, the macroscopic concentration gradients invoked in refs 43 and 44 are difficult to justify for systems at equilibrium like those studied in refs 13 and 23 and in the present work. The group of Langevin[21] has suggested that negative effective values of $\kappa(\omega)$ might be linked to the existence of surface-phase transitions. Noskov and Loglio[8] and Muñoz et al.[22] have suggested that these anomalous viscosities may be linked to the fact that the dispersion equation (eq 6) does not take into account all the hydrodynamic modes relevant for real interfaces.

The presence of inert electrolyte strongly reduces the thickness of the electrical double layer,[16] making the Debye length $\zeta^{-1}$ comparable to the penetration length of the capillary wave $\mu^{-1}$. A possible consequence is that, at the high frequencies studied in this work, the penetration of the capillary wave may disturb the equilibrium distribution of surfactant ions, thus leading to a concentration gradient similar to the one recently considered by Hennenberg et al.[45] This would lead to a new contribution to the restoration forces of the capillary mode and thus to new terms in the dispersion equation. This new contribution should be smaller for the case in which $\zeta^{-1} \gg \mu$.

**An Extended Dispersion Equation.** Hennenberg et al.[45] have stated that surface renewal is due to both interfacial compressibility and shape deformation playing together; then, capillary deformation of the interface brings the monolayer into contact with bulk regions with different surfactant concentration (or electrostatic potential). Hence, the Marangoni force (surface tension gradients) caused mainly by surface dilation (see eq 3) contains now an additional term proportional to the transversal velocity $v_z = du_z/dt$ through a new additional elastic constant $\epsilon_2$:

$$\delta\gamma = \tilde{\epsilon}\frac{\partial u_x}{\partial x} + \epsilon_2 v_z \tag{21}$$

The first term, proportional to the dilational viscoelastic modulus $\tilde{\epsilon}(\omega)$, is the only one explicitly considered in the LT model and in the classical hydrodynamic frame to counterbalance the longitudinal stress in a flat interface (see eq 3). The second term, characterized by the new viscoelastic coefficient, $\epsilon_2(\omega)$, can be interpreted as a shape-compression coupling contribution to the elastic free energy of the interface. The free-energy functional in eq 1 must be rewritten now as

$$\delta F = \frac{1}{2}\tilde{\gamma}\left(\frac{\partial u_z}{\partial x}\right)^2 + \frac{1}{2}\tilde{\epsilon}\left(\frac{\partial u_x}{\partial x}\right)^2 + \epsilon_2\left(\frac{\partial u_x}{\partial x}\right)\left(\frac{\partial u_z}{\partial x}\right) \tag{22}$$

that is, the new term couples transversal deformation, caused by the capillary wave, with longitudinal dilation of the interface through the coefficient $\epsilon_2$. This is an important difference with the classical Levich−Lucassen hydrodynamic treatment of a viscoelastic monolayer,[5−8] where the coupling between the two types of modes is indirect through the bulk phases. In general, this non-hydrodynamic coupling term can be thought of as a compositional coupling between capillary and dilational modes, which is independent of the hydrodynamic coupling given by the term $C(\rho,\eta)$ in eqs 6 and 10. As a result, the dispersion equation for surface motion maintains the same structure as in the classical Levich's one (eq 6), but it appears now modified by this extra compositional coupling characterized by $\epsilon_2$; eq 22 leads to the following dispersion equation:

$$D(\omega) = L(\gamma)\cdot T(\tilde{\epsilon}) - C_H(\rho,\eta;\epsilon_2) \equiv 0 \tag{23}$$

where the longitudinal ($L$) and transversal ($T$) terms are the same as in eqs 7 and 8, respectively.

Now, the coupling term is

$$C_H(\rho,\eta;\epsilon_2) = [i\omega\eta(q-\mu) + \epsilon_2 q^2]^2 \tag{24}$$

Notice that if $\epsilon_2 = 0$, eq 24 reduces to eq 10. The effect of $\epsilon_2$ is to increase the coupling between capillary and dilational modes. As a consequence, when fitting SQELS spectra, the effect of $\epsilon_2 > 0$ is qualitatively similar to that of negative effective values of the dilational viscosity, $\kappa < 0$. This is illustrated in Figure 8 where the experimental spectrum for DAC ($c = 0.009$ mM) + water + KCl (60 mM) is plotted together with the best fits to the theoretical spectra from the classical dispersion equation (eq 6) and the one modified here (eq 23). When $\kappa$ is restricted to positive values or zero, the classical spectrum is not able to fit the experimental one. Similar results are found for the whole concentration range. Figure 9 shows the viscoelastic parameters obtained at $c = 0.009$ mM as a function of frequency. As already said, eq 6 leads to $\kappa(\omega) < 0$ and positive values of $\epsilon(\omega)$ in quantitative disagreement with the MLT−FD model. However, eq 23 leads to values of $\epsilon(\omega)$ which are, within their uncertainties, independent of the frequency and close to the value of the Gibbs compression modulus, $\epsilon_0$. This behavior is expected in the high-frequency limit, where the monolayer behaves as insoluble ($\Omega \sim 0$ in the LT model).

We have found $\epsilon_2$ values which are moderately high, about the same magnitude as $\epsilon_0$, for the whole concentration range. A quantitative interpretation of $\epsilon_2$ in terms of the internal

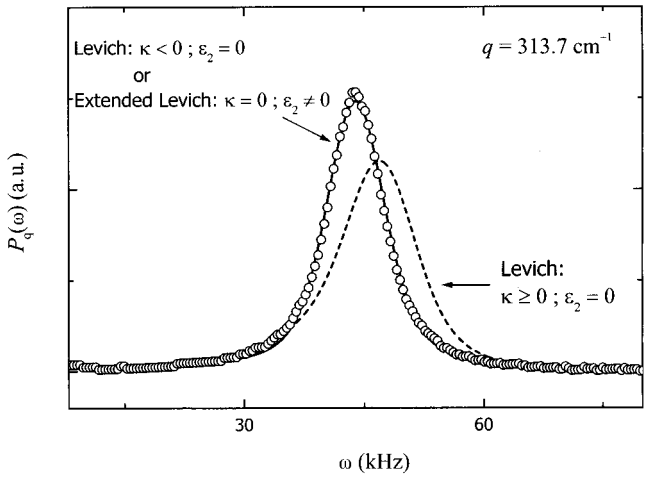


**Figure 8.** SQELS spectrum for a monolayer of the DAC ($c = 0.009$ mM) + water + KCl (60 mM) system at $q = 313.7$ cm$^{-1}$. The curves are predictions of the extended dispersion equation (eq 27). When the new coupling parameter $\epsilon_2 = 0$ (i.e., the classical Levich's dispersion equation), it is not possible to fit the experimental spectra unless $\kappa < 0$ is allowed. However, good fits can be obtained with $\epsilon_2 \neq 0$ without having to use unphysical values of $\kappa$.

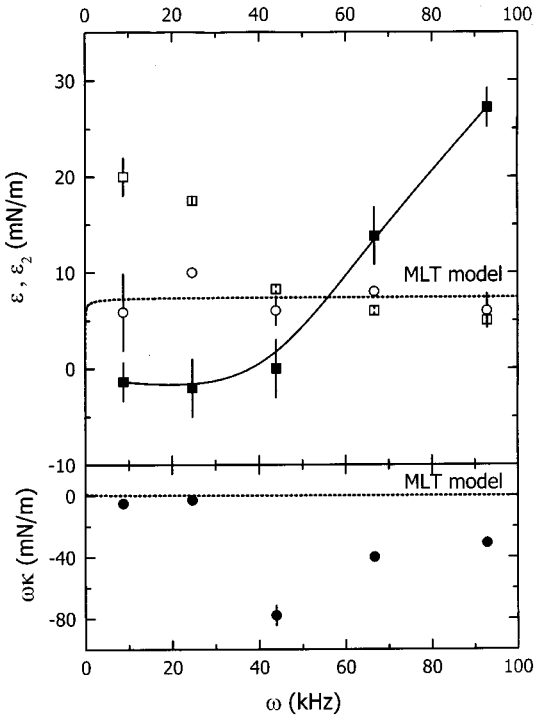


**Figure 9.** (a) Frequency dependence of dynamic dilational elasticity $\epsilon(\omega)$ and of the coupling constant $\epsilon_2$ for the system DAC (0.009 mM) + water + KCl (60 mM). (b) Dilational loss modulus. Solid symbols correspond to the classical analysis with $\epsilon_2 = 0$; this dispersion equation leads to negative values of $\omega\kappa(\omega)$ and to a frequency dependence of the loss modulus which is in disagreement with the predictions of the MLT model (dashed line). Open symbols correspond to the values of the elastic constants when $\kappa$ is set to zero: (○) dilational elasticity modulus $\epsilon(\omega)$, and (□) coupling constant $\epsilon_2$.

structure of the monolayer and the interfacial region is still lacking, thus it is difficult to make further comments on the present preliminary results. In addition, one should not forget that possible effects of electrostatics to the free-energy functional (eq 22) have not been considered.

## Conclusions

Equilibrium surface-tension data obtained for the DAC + water system have been analyzed in terms of the Frumkin−Davies equation of state, which incorporates electrostatic interactions. This analysis leads to adsorption values compatible with the ones obtained from the Gibbs' law. In addition, reasonable electrostatic surface potentials $\Psi_0$ are obtained from this approach as a function of surfactant concentration. It saturates at a concentration near the CMC where adsorption does. When salt is added, CMC is lowered as expected since charges are screened; the monolayer becomes denser at lower bulk surfactant concentrations. In this case, smaller values of $\Psi_0$ are obtained from the analysis of the equilibrium surface tensions in terms of the FD isotherm, as expected from a screened system. This equilibrium behavior is compatible with the existence of an electrostatic adsorption barrier which will be partially inhibited with the addition of salt.

The dilational viscoelasticity of the adsorbed monolayers have been obtained from the analysis of the SQELS spectra of the capillary waves. In the salt-free case, both the dilational elasticity and viscosity can be well described by the classical Lucassen−van den Tempel model if an adsorption barrier is properly accounted for (MLT model). When the electrostatic barrier is inhibited (by addition of salt, KCl 60 mM), negative values of the dilational viscosity are obtained from the analysis in terms of the classical hydrodynamic frame. Following Hennenberg's argument, an additional internal coupling between dilational and capillary modes has been included into the hydrodynamic equations. The analysis of the experimental SQELS spectra in terms of this extended dispersion equation removes this unphysical situation and leads to dilational viscoelastic parameters compatible with the equilibrium value and with the $\omega$-dependence expected from the MLT model. This system seems well suited to further explore the appearance of this pathological behavior because we can switch from regular to anomalous dilational viscoelasticity by tuning the solution ionic strength.

**Acknowledgment.** This work was supported in part by MCYT under grant BQU2000-0786 and by Fundación Ramón Areces. The work of M.G. Muñoz is supported by a fellowship from U.C.M. F. Monroy is grateful to D. Langevin for many stimulating discussions.

## References and Notes

(1) Safran, S. A. *Statistical Thermodynamics of Surfaces, Interfaces, and Membranes*; Addison-Wesley: Reading, MA, 1994.
(2) Fennell-Evans, D.; Wennestrom, H. *The Colloidal Domain*; Wiley-VCH: New York, 1999.
(3) Lucassen-Reynders, E. H.; Lucassen, J. *Adv. Colloid Interface Sci.* **1969**, *2*, 347. Djabbarah, N. F.; Wassan, D. T. *Chem. Eng. Sci*. **1982**, *37*, 175.
(4) Dickinson, E. *J. Food Eng.* **1994**, *22*, 59.
(5) *Light Scattering by Liquid Surfaces and Complementary Techniques*; Langevin, D., Ed.; Surfactant Science Series, Vol. 41; Marcel Dekker: New York, 1992.
(6) Buzza, D. M. A.; Jones, J. L.; McLeish, T. C. B.; Richards, R. W. *J. Chem. Phys.* **1998**, *109*, 5008.
(7) Levich, B. G. *Physicochemical Hydrodynamics*; Prentice-Hall: NJ, 1962.
(8) Noskov, B.; Loglio, G. *Colloids Surf., A* **1998**, *143*, 167.
(9) Lucassen, J.; van den Tempel, M. *Chem. Eng. Sci.* **1972**, *271*, 1283; *J. Colloid Interface Sci.* **1972**, *41*, 491.
(10) van den Tempel, M.; Luscassen-Reynders, E. H. *Adv. Colloid Interface Sci.* **1983**, *18*, 281.
(11) Eastoe, J.; Dalton, J. S. *Adv. Colloid Interface Sci.* **2000**, *85*, 103
(12) Lemaire, C.; Langevin, D. *Colloids Surf., A* **1992**, *65*, 101.
(13) Bonfillon, A.; Langevin, D. *Langmuir* **1992**, *9*, 8; **1994**, *10*, 2965.
(14) Prosser, A. J.; Franses, E. I. *Colloids Surf., A* **2001**, *178*, 1.
(15) Datwani, S. S.; Stebe, K. J. J. *Colloid Interface Sci*. **1999**, *219*, 282.
(16) MacLeod, C. A.; Radke, C. J. *Langmuir* **1994**, *10*, 3555.
(17) Waszynsky, P.; Wantke, K. D.; Fruhner, H. *Colloids Surf.* **2001**, *189*, 29.
(18) Earnshaw, J. C.; McCoo, E. *Langmuir* **1995**, *11*, 1087.
(19) Monroy, F.; Giermanska-Kahn, J.; Langevin, D. J. *non-Equil. Thermodyn*. **2000**, *25*, 279.
(20) Earnshaw, J. C.; McCoo, E. *Phys. Rev. Lett.* **1994**, *72*, 84.
(21) Giermanska-Kahn, J.; Monroy, F.; Langevin, D. *Phys. Rev. E* **1999**, *60*, 7163.
(22) Muñoz, M. G.; Luna, L.; Monroy, F.; Rubio, R. G.; Ortega, F. *Langmuir* **2000**, *16*, 6657.
(23) Sharpe, D.; Eastoe, J. *Langmuir* **1996**, *12*, 2303.
(24) Martín, A.; López, I.; Monroy, F.; Casielles, A. G.; Ortega, F.; Rubio, R. G. *J. Chem. Phys.* **1994**, *101*, 6874.
(25) Martín, A.; Casielles, A. G.; Muñoz, M. G.; Ortega, F.; Rubio, R. G. *Phys. Rev. E* **1998**, *58*, 2151.
(26) Motomura, K.; Iwanaga, S. I.; Hayami, Y.; Uryu, S.; Matuura, R. J. *Colloid Interface Sci*. **1981**, *80*, 32.
(27) Kizling, J.; Stenius, P.; Eriksson, J. Ch.; Ljunggren, S. *J. Colloid Interface Sci*. **1995**, *171*, 162.
(28) Byrne, D.; Earnshaw, J. C. *J. Phys. D: Appl. Phys*. **1979**, *12*, 1145.
(29) Monroy, F.; Ortega, F.; Rubio, R. G. *Phys. Rev. E* **1998**, *58*, 7629.
(30) Dorshow, R. B.; Bunton, C. A.; Nicoli, D. F. In *Surfactants in Solution*; Mittal, K. L., Bothorel, P., Eds.; Plenum: New York, 1986, Vol. 4.
(31) Monroy, F.; Ortega, F.; Rubio, R. G. *J. Phys. Chem. B* **1999**, *103*, 2061.
(32) Davies, J. T.; Rideal, E. *Interfacial Phenomena*; Academic Press: London, 1961.
(33) Borwankar, R. P.; Wasan, D. T. *Chem. Eng. Sci*. **1988**, *43*, 1323.
(34) Strey, R.; Viisanen, Y.; Aratono, M.; Kratohvil, J. P.; Yin, Q.; Friberg, S. E. *J. Phys. Chem.* **1999**, *103*, 9112.
(35) *Cationic Surfactants*; Rubingh, D. N., Holland, P. M., Eds.; Surfactant Science Series, Vol. 34; Marcel Dekker: New York, 1991.
(36) Israelachvili, J. *Intermolecular and Surface Forces*; Academic Press: London, 1991.
(37) Marcus, Y. *Ion Solvation*; Wiley-Interscience: Chichester, U.K., 1985.
(38) Eastoe, J.; Dalton, J. S. *Adv. Colloid Interface Sci.* **2000**, *85*, 103.
(39) Ravera, F.; Liggieri, L.; Steinchen, A. *J. Colloid Interface Sci.* **1993**, *156*, 109.
(40) Liggieri, L.; Ravera, F.; Passerone, A. *Colloids Surf., A* **1996**, *114*, 351.
(41) Monroy, F.; Giermanska-Kahn, J.; Langevin, D. *Colloids Surf., A* **1998**, *143*, 251.
(42) Li, B.; Geeraerts, G.; Joos, P. *Colloids Surf., A* **1994**, *88*, 251.
(43) Hennenberg, M.; Chu, X.-L.; Sanfeld, A.; Velarde, M. G. *J. Colloid Interface Sci.* **1982**, *150*, 7.
(44) Chu, X.-L.; Velarde, M. G. *Physicochem. Hydrodynam*. **1988**, *10*, 727.
(45) Hennenberg, M.; Slavtchev, S.; Weyssow, B.; Legros, J.-C. *J. Colloid. Interface Sci.* **2000**, *230*, 216.